Dilithioplumbole: A Lead-Bearing Aromatic Cyclopentadienyl Analog

Masaichi Saito, *et al.*

Science **328**, 339 (2010);
DOI: 10.1126/science.1183648

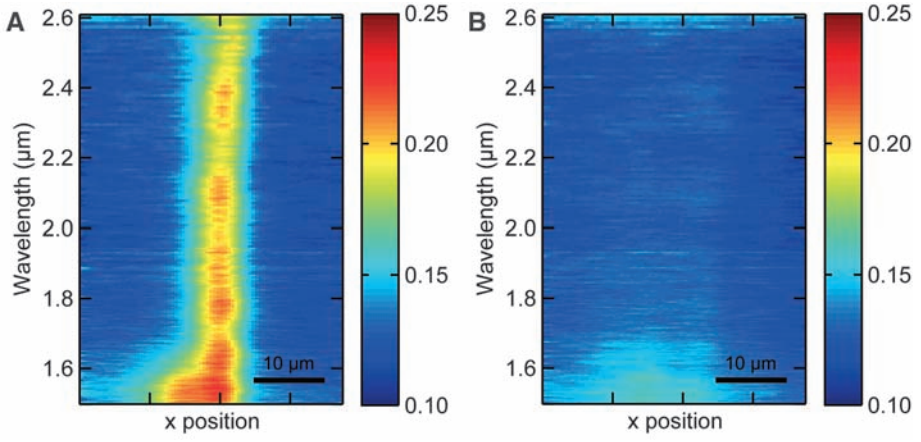

Fig. 4. Optical characterization of the 3D structures with unpolarized light as in Fig. 3, but in dark-field mode. (**A**) The bump is immediately visible by enhanced scattering. (**B**) Scattering is largely reduced with the cloak.

derived from the quasi-conformal mapping in transformation optics to obtain good invisibility-cloaking performance.

Finally, Fig. 4 depicts data taken in dark-field mode from 1.5- to 2.6-μm wavelengths (data over a larger spectral interval are shown in fig. S4). Here, the same sample as in Fig. 3 is tilted such that the optical axis lies within the *xy* plane and includes an angle of 35° with the *y* axis. As usual for the dark-field mode, the collected light results from scattering by the sample. These data are normalized with respect to a normal-incidence reflection spectrum taken on the gold film. The bump without cloak in Fig. 4A is immediately visible. We assign this finding to enhanced scattering from the illuminated side of the bump. The visibility is again drastically reduced for the case of bump with cloak in Fig. 4B.

References and Notes

1. J. B. Pendry, D. Schurig, D. R. Smith, *Science* **312**, 1780 (2006); published online 25 May 2006 (10.1126/science.1125907).
2. U. Leonhardt, *Science* **312**, 1777 (2006); published online 25 May 2006 (10.1126/science.1126493).
3. U. Leonhardt, T. G. Philbin, *New J. Phys.* **8**, 247 (2006).
4. U. Leonhardt, *New J. Phys.* **8**, 118 (2006).
5. D. Schurig *et al.*, *Science* **314**, 977 (2006); published online 19 October 2006 (10.1126/science.1133628).
6. W. Cai, U. K. Chettiar, A. V. Kildishev, V. M. Shalaev, *Nat. Photonics* **1**, 224 (2007).
7. V. M. Shalaev, *Science* **322**, 384 (2008).
8. J. Li, J. B. Pendry, *Phys. Rev. Lett.* **101**, 203901 (2008).
9. U. Leonhardt, T. Tyc, *Science* **323**, 110 (2009); published online 20 November 2008 (10.1126/science.1166332).
10. R. Liu *et al.*, *Science* **323**, 366 (2009).
11. J. Valentine, J. Li, T. Zentgraf, G. Bartal, X. Zhang, *Nat. Mater.* **8**, 568 (2009).
12. L. H. Gabrielli, J. Cardenas, C. B. Poitras, M. Lipson, *Nat. Photonics* **3**, 461 (2009).
13. J. H. Lee *et al.*, *Opt. Express* **17**, 12922 (2009).
14. I. I. Smolyaninov, V. N. Smolyaninova, A. V. Kildishev, V. M. Shalaev, *Phys. Rev. Lett.* **102**, 213901 (2009).
15. G. W. Milton, N. A. P. Nicorovici, *Proc. R. Soc. London Ser. A* **462**, 3027 (2006).
16. A. Alù, N. Engheta, *Phys. Rev. E* **72**, 016623 (2005).
17. J. C. Halimeh, T. Ergin, J. Mueller, N. Stenger, M. Wegener, *Opt. Express* **17**, 19328 (2009).
18. See supporting material available on *Science* Online.
19. K. M. Ho, C. T. Chan, C. M. Soukoulis, R. Biswas, M. Sigalas, *Solid State Commun.* **89**, 413 (1994).
20. M. Deubel *et al.*, *Nat. Mater.* **3**, 444 (2004).
21. S. G. Johnson, J. D. Joannopoulos, *Opt. Express* **8**, 173 (2001).
22. S. Kawata, H.-B. Sun, T. Tanaka, K. Takada, *Nature* **412**, 697 (2001).

23. We thank K. Busch, G. von Freymann, S. Linden, and M. Thiel for discussions and help regarding sample fabrication and photonic band-structure calculations. We acknowledge support from the Deutsche Forschungsgemeinschaft (DFG) and the State of Baden-Württemberg through the DFG–Center for Functional Nanostructures within subprojects A1.4 and A1.5. We also thank the Future and Emerging Technologies (FET) program within the Seventh Framework Programme for Research of the European Commission (FET open grant number 213390) for financial support of the project PHOME. The project METAMAT is supported by the Bundesministerium für Bildung und Forschung. The Ph.D. education of T.E. is embedded in the Karlsruhe School of Optics and Photonics (KSOP); N.S. is supported as a mentor in the KSOP.

Supporting Online Material

www.sciencemag.org/cgi/content/full/science.1186351/DC1
SOM Text
Figs. S1 to S5

23 December 2009; accepted 4 March 2010
Published online 18 March 2010;
10.1126/science.1186351
Include this information when citing this paper.

Dilithioplumbole: A Lead-Bearing Aromatic Cyclopentadienyl Analog

Masaichi Saito,[1]* Masafumi Sakaguchi,[1] Tomoyuki Tajima,[1] Kazuya Ishimura,[2] Shigeru Nagase,[2] Masahiko Hada[3]

Although the concept of aromaticity has long played an important role in carbon chemistry, it has been unclear how applicable the stabilizing framework is to the heaviest elements. Here we report the synthesis of dilithiotetraphenylplumbole by reduction of hexaphenylplumbole. X-ray crystallography revealed a planar structure with no alternation of carbon–carbon bond lengths in the five-membered ring core. Nuclear magnetic resonance spectra and relativistic theoretical calculations show considerable aromatic character in the molecule, thus extending aromaticity to carbon's heaviest congener.

Aromaticity has been a fundamental chemical concept since the discovery of benzene in 1825, and aromatic compounds have long played important roles in all fields of chemistry. The skeletons of most aromatic compounds consist of C atoms, and occasionally N, O, and the third-row elements S and more rarely P. To determine whether the heavier group-14 elements could sustain aromaticity, Si and Ge analogs of carbocyclic aromatic compounds such as benzene, naphthalene (*1*, *2*), cyclopentadienyl anion (*3*–*7*), cyclobutadiene dianion (*8*), and cyclopropenyl cation (*9*–*12*) have recently been synthesized, in which one ring C is replaced by the congener. Most of these have considerable aromatic character, even though some of them have been judged nonaromatic because of their nonplanar structures. Most recently, dilithiostannole (*13*) and 2-stannanaphthalene (*14*) have been synthesized and concluded to be aromatic compounds. Therefore, the concept of aromaticity has been expanded to Sn-containing carbocyclic systems. However, there has been no experimental evidence of whether the concept of aromaticity can be expanded to Pb-containing C rings, even though theoretical calculations predicted that dilithioplumbole would have considerable aromatic character (*15*, *16*). We report here the synthesis of dilithiotetraphenylplumbole, thus expanding the concept of aromaticity to C cycles incorporating the heaviest group-14 element (*17*).

The synthesis of dilithiotetraphenylplumbole **1** was accomplished by the reduction of hexa-

[1]Department of Chemistry, Graduate School of Science and Engineering, Saitama University, Shimo-okubo, Sakura-ku, Saitama-city, Saitama, 338-8570 Japan. [2]Department of Theoretical Molecular and Computational Science, Institute for Molecular Science, Myodaiji, Okazaki, Aichi, 444-8585 Japan. [3]Department of Chemistry, Graduate School of Science and Engineering, Tokyo Metropolitan University, Minami-osawa, Hachiohji, Tokyo, 192-0397 Japan.

*To whom correspondence should be addressed. E-mail: masaichi@chem.saitama-u.ac.jp

phenylplumbole **2** (*18*) with lithium in the presence of a catalytic amount of naphthalene in ether at −78°C; a byproduct, phenyllithium, was also formed (*19*). After treatment of the reaction mixture with dimethoxyethane (DME), the phenyllithium fully decomposed, and dilithioplumbole **1** was isolated in 78% yield (Fig. 1A). The molecular structure of dilithioplumbole **1** was established by x-ray crystallographic analysis (Fig. 1B). One Li atom is coordinated by the plumbole ring in an η^5 fashion, whereas the other Li atom is coordinated by three DME molecules. Because the distance between the Pb and DME-solvated Li atoms is more than 10 Å, the solvated Li atom has no interaction with the plumbole ring. The plumbole ring is planar with a 539.8° sum of the internal angles. The C–C distances within the ring are almost equal [1.410(6), 1.412(6), and 1.431(6) Å], as was observed in the aromatic dilithiostannole, suggesting that dilithioplumbole **1** has considerable aromatic character. In contrast, the C–C bonds of the starting plumbole **2** differ [1.345(6), 1.354(5), and 1.522(5) Å] (*18*). The Pb–C bonds of **1** lengthen to 2.242(4) and 2.265(5) Å, compared with those of **2** [2.202(4) and 2.211(4) Å], resulting in a smaller C–Pb–C angle [75.97(17)°] than in **2** [82.41(14)°].

In the ^{13}C nuclear magnetic resonance (NMR) spectrum of **1**, a signal assignable to the α C was observed at 228 parts per million (ppm), which is a substantial downfield shift as compared with the corresponding resonance in **2** (154 ppm); whereas the β C of **1** resonated at 147 ppm, a slight upfield shift relative to **2** (153 ppm). This trend was also observed in the cases of other aromatic group-14 dilithiometalloles (*13*). In contrast, the resonance of the β C of lithiotriphenylplumbane, which is not aromatic, shifts downfield relative to the tetraphenylplumbane precursor (*20*). This NMR analysis also suggests that dilithioplumbole **1** has considerable aromatic character. Although the upfield resonance in the ^{7}Li NMR spectrum is diagnostic of the aromatic ring current, the ^{7}Li NMR signal of **1** was observed at −1.11 ppm, which is in the range of normal organolithium compounds, suggesting that rapid exchange of η^5-coordinated and solvent-coordinated Li cations is occurring in solution. The ^{207}Pb NMR signal of **1** was observed at 1712.8 ppm, remarkably downfield of the signal in the spectrum of **2** (−24.5 ppm) (*18*). The corresponding shifts in the ^{207}Pb NMR spectra of tetraphenylplumbane and lithiotriphenylplumbane are −179 and 1060.1 ppm, respectively (*20*). The downfield ^{207}Pb shift of **1** relative to lithiotriphenylplumbane is probably due to greater anionic character of the lead atom of **1** or some contribution of plumbylene character. A similar contribution of divalent character in the dilithiometalloles has already been proposed (*13*, *21*).

To gain more insight into the structure and electronic states of dilithioplumbole **1**, theoretical calculations were carried out (*22*). Because the x-ray structural analysis of **1** revealed that one of the Li atoms is coordinated by the plumbole ring and the other is separated from the ring, geometric optimization of the dilithioplumbole **3** was carried out at the B3LYP (*23*, *24*) level with the second-order Douglas-Kroll-Hess scalar relativistic term (*25*–*27*) (Fig. 2). The ANO-RCC basis set (*28*) was adopted for Pb. The [6*s*6*p*5*d*1*f*] functions were picked out from the original [11*s*10*p*9*d*8*f*4*g*] functions, and each valence-contracted function was then split into three functions of triple-zeta quality. Furthermore, the functions for 1*s* and 2*p* orbitals were doubly uncontracted to describe the relativistic correction of the inner core region. A polarization *d* function was not added because the exponent was close to that of the uncontracted function described above. The final contraction form was [9*s*9*p*7*d*3*f*]. The 6-311G(2d) basis set (*29*) was used for Li atoms and for C and H atoms of the five-membered ring and those connected to the ring and the Li atoms, whereas the 6-31G basis set (*30*) was used for other C and H atoms. The optimized geometry of **3** was highly consistent with the x-ray structure of **1**. The Pb–C(α), C(α)–C(β), and C(β)–C(β) bond distances were calculated to be (2.292, 2.304), (1,411, 1,429), and 1.452 Å, respectively. The Pb–C(α) bonds of **1** were elongated as compared with those of **2**, even though aromatization usually results in elongation and shortening of the original double and single bonds, respectively. To understand this contradiction, geometric optimization of the model compounds C_4H_6M, C_4H_4M, and $C_4H_4M^{2-}$ (M = Si, Ge, Sn,

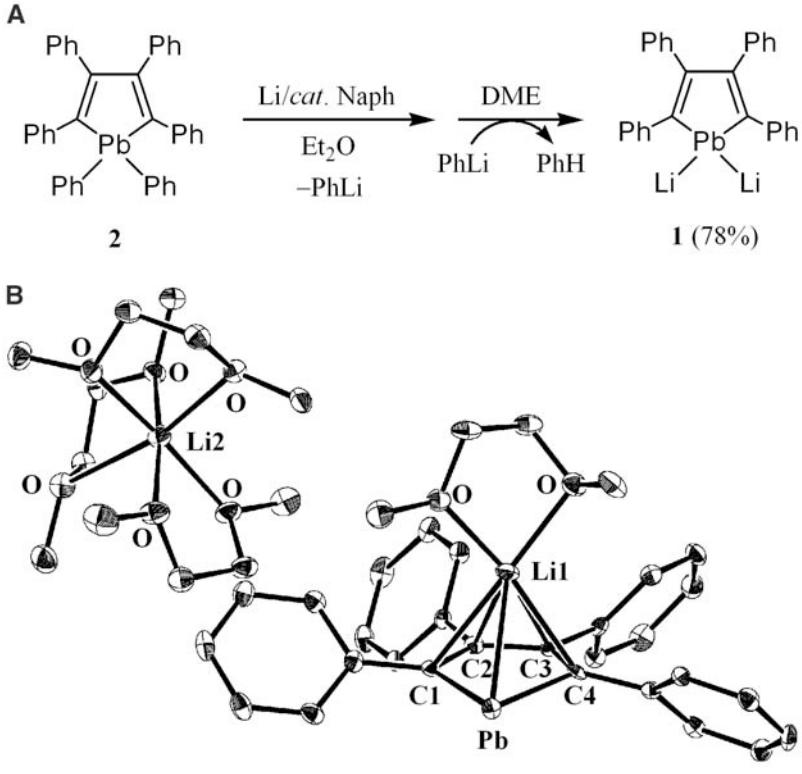

Fig. 1. (**A**) Preparation of dilithiotetraphenylplumbole **1**. (**B**) ORTEP drawing of dilithiotetraphenylplumbole **1** with thermal ellipsoids plots drawn at 40% probability for non-H atoms. All H atoms were omitted for clarity. Selected bond lengths (angstroms) and angles (degrees) are as follows: Pb–C1, 2.242(4); Pb–C4, 2.265(5); C1–C2, 1.410(6); C2–C3, 1.431(6); C3–C4, 1.412(6); and C1–Pb–C4, 75.99(17)

Fig. 2. Comparison of the structures of **1**·4DME and **3**.

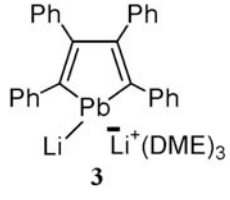

	Crystal structure of **1**·4DME	Calculation of **3**
Pb–C(α)	2.242(4), 2.265(5) Å	2.292, 2.304 Å
C(α)–C(β)	1.410(6), 1.412(6) Å	1.411, 1.429 Å
C(β)–C(β)	1.431(6) Å	1.452 Å

or Pb) was carried out at the B3LYP level using the LanL2DZ basis set (*31*, *32*) (Fig. 3). In the transition from C_4H_6Pb to C_4H_4Pb, which has a divalent Pb atom, the Pb–C(α) bond lengthened from 2.175 to 2.256 Å; whereas in the transition from C_4H_4Pb to $C_4H_4Pb^{2-}$, the corresponding bond shortened to 2.240 Å [2.242(4) and 2.265(5) Å are the two Pb–C(α) bond lengths in **1**]. The elongation of the Pb–C(α) bond from C_4H_6Pb to C_4H_4Pb can reasonably be attributed to an increase in the *p* character of the Pb–C(α) bond caused by a lone pair on the Pb atom having more *s* character than the Pb–H bonds of C_4H_6Pb. In contrast, the shortening of the Pb–C(α) bond from C_4H_4Pb to $C_4H_4Pb^{2-}$ can be attributed to aromatic delocalization of the negative charges. This trend was also observed in all of the heavier group-14 metalloles, even though the Si–C(α) bond of C_4H_6Si is comparable to that of $C_4H_4Si^{2-}$ (Fig. 3).

NMR chemical shifts of dilithioplumbole **1** were also calculated on the basis of the x-ray structure. Relativistic effects were found to be essential for accurate calculations. When they were included, $^{13}C(\alpha)$ and ^{207}Pb chemical shifts of 220.7 and 1655.9 ppm were calculated, which were highly consistent with the experimental values (228.33 and 1712.8 ppm, respectively). Under nonrelativistic conditions, the calculations yielded the considerably less accurate shifts 269.0 and 38110.1 ppm. The Li nucleus above the aromatic plumbole ring was calculated to resonate about 4 ppm higher than the Li nucleus coordinated by three DME molecules. The experimental ^{7}Li NMR chemical shift of −1.11 ppm was therefore suggestive of rapid exchange of the two inequivalent Li cations in solution. The considerably negative NICS(1) (*33*) value of a free plumbole anion was calculated to be −6.28 ppm, suggesting that dilithioplumbole **1** is also aromatic, as the other group-14 dilithiometalloles are.

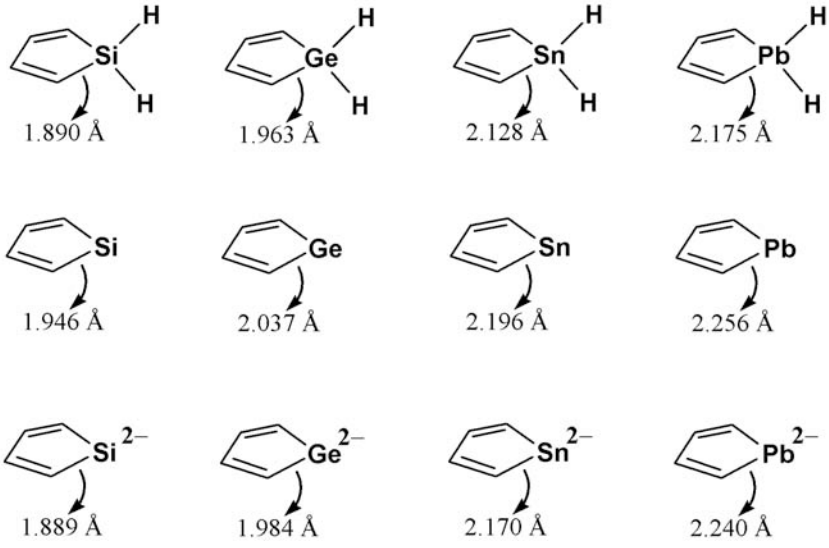

Fig. 3. Comparison of the calculated M–C(α) bond lengths in group-14 metalloles.

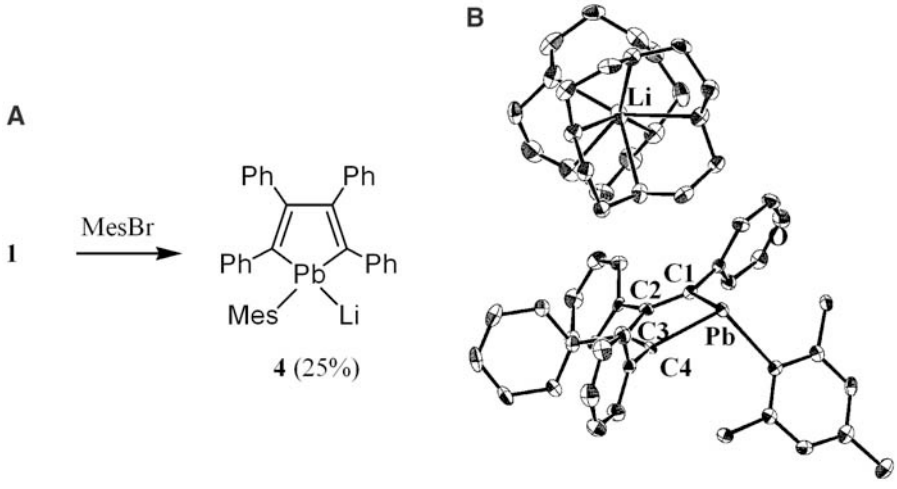

Fig. 4. (**A**) Reaction of **1** with bromomesitylene to afford lithiomesitylplumbole **4**. (**B**) ORTEP drawing of lithiomesitylplumbole **4** with thermal ellipsoids plots drawn at 40% probability for non-H atoms. All H atoms were omitted for clarity. Selected bond lengths (angstroms) and angles (degrees) are as follows: Pb–C1, 2.320(5); Pb–C4, 2.306(5); C1–C2, 1.354(8); C2–C3, 1.498(8); C3–C4, 1.347(8); and C1–Pb–C4, 75.7(2).

Dilithioplumbole **1** reacted with bromomesitylene to give lithiomesityltetraphenylplumbole **4** in 25% yield (Fig. 4A) (*19*). The ^{207}Pb NMR signal of **4** was observed at 1095.7 ppm, comparable to that of lithiotriphenylplumbane (1060.1 ppm) (*10*). The structure of lithiomesitylplumbole **4** was established by x-ray diffraction analysis (Fig. 4B) after crystallization with 12-crown-4. The Li atom is coordinated by two molecules of crown ether, and the distance between the Li and the Pb atoms of more than 6 Å suggests no interaction between them. The C–C bonds within the plumbole ring of **4** differ [1.347(8), 1.498(8), and 1.354(8) Å]. The pyramidalization of the Pb center is clearly evident from the angle between the plumbole ring and the Pb–C(mesityl) bond of 103.4°. These geometric features clearly show that lithiomesitylplumbole **4** is nonaromatic, even though the plumbole ring is planar with a sum of internal angles of 539.8°.

The present findings show decisively that 2*p*(C) and 6*p*(Pb) orbitals can overlap sufficiently to create aromatic molecules. We believe that the present dilithioplumbole highlights the future possibility of introducing heavy elements including Pb into a broader range of C frameworks, providing compounds with structures and properties that are applicable to catalytic and materials chemistry.

References and Notes

1. N. Tokitoh, *Acc. Chem. Res.* **37**, 86 (2004).
2. N. Tokitoh, *Bull. Chem. Soc. Jpn.* **77**, 429 (2004).
3. J. Dubac, C. Guérin, P. Meunier, in *The Chemistry of Organic Silicon Compounds*, Z. Rappoport, Y. Apeloig, Eds. (Wiley, Chichester, UK, 1998), pp. 1961–2036.
4. M. Saito, M. Yoshioka, *Coord. Chem. Rev.* **249**, 765 (2005).
5. V. Y. Lee, A. Sekiguchi, *Angew. Chem. Int. Ed.* **46**, 6596 (2007).
6. Most recently, heavier congeners of the cyclopentadienyl anion incorporating more than two heavy group-14 atoms have been found to be aromatic (*7*, *34*).
7. H. Yasuda, V. Y. Lee, A. Sekiguchi, *J. Am. Chem. Soc.* **131**, 6352 (2009).
8. V. Y. Lee, K. Takanashi, T. Matsuno, M. Ichinohe, A. Sekiguchi, *J. Am. Chem. Soc.* **126**, 4758 (2004).
9. A. Sekiguchi, M. Tsukamoto, M. Ichinohe, *Science* **275**, 60 (1997).
10. M. Ichinohe, M. Igarashi, K. Sanuki, A. Sekiguchi, *J. Am. Chem. Soc.* **127**, 9978 (2005).
11. M. Igarashi, M. Ichinohe, A. Sekiguchi, *J. Am. Chem. Soc.* **129**, 12660 (2007).
12. X. W. Li, W. T. Pennington, G. H. Robinson, *J. Am. Chem. Soc.* **117**, 7578 (1995).
13. M. Saito, R. Haga, M. Yoshioka, K. Ishimura, S. Nagase, *Angew. Chem. Int. Ed.* **44**, 6553 (2005).
14. Y. Mizuhata, T. Sasamori, N. Takeda, N. Tokitoh, *J. Am. Chem. Soc.* **128**, 1050 (2006).
15. B. Goldfuss, P. R. Schleyer, F. Hampel, *Organometallics* **15**, 1755 (1996).
16. B. Goldfuss, P. R. Schleyer, *Organometallics* **16**, 1543 (1997).
17. Although the synthesis of 4-*t*-butylbismabenzene, which contains the heaviest stable element bismuth, was reported, the compound was stable for several hours at 0°C only in solution, and the solid-state structure was not reported (*35*).

18. M. Saito, M. Sakaguchi, T. Tajima, K. Ishimura, S. Nagase, *Phosphorus Sulfur Silicon Relat. Elem.* 10.1080/10426501003773399 (2010).
19. Methods are detailed in supporting material available on *Science* Online.
20. U. Edlund, T. Lejon, P. Pyykkö, T. K. Venkatachalam, E. Buncel, *J. Am. Chem. Soc.* **109**, 5982 (1987).
21. J.-H. Hong, P. Boudjouk, S. Castellino, *Organometallics* **13**, 3387 (1994).
22. All calculations were performed with Gaussian 03 revision D.02 (*36*).
23. A. D. Becke, *J. Chem. Phys.* **98**, 5648 (1993).
24. C. Lee, W. Yang, R. G. Parr, *Phys. Rev. B* **37**, 785 (1988).
25. M. Douglas, N. M. Kroll, *Ann. Phys.* **82**, 89 (1974).
26. B. A. Hess, *Phys. Rev. A* **32**, 756 (1985).
27. B. A. Hess, *Phys. Rev. A* **33**, 3742 (1986).
28. B. O. Roos, R. Lindh, P.-Å. Malmqvist, V. Veryazov, P.-O. Widmark, *J. Phys. Chem. A* **108**, 2851 (2004).
29. R. Krishnan, J. S. Binkley, R. Seeger, J. A. Pople, *J. Chem. Phys.* **72**, 650 (1980).
30. W. J. Hehre, R. Ditchfield, J. A. Pople, *J. Chem. Phys.* **56**, 2257 (1972).
31. W. R. Wadt, P. J. Hay, *J. Chem. Phys.* **82**, 284 (1985).
32. T. H. Dunning Jr., P. J. Hay, *Methods of Electronic Structure Theory*, Vol. 2, H. F. Schaefer III, Ed. (Plenum, New York, 1977).
33. The NICS, which is an abbreviation of nucleus-independent chemical shifts, was first proposed as a probe of aromaticity on the basis of magnetic criteria (*37*) and is now generally used to characterize the aromaticity of compounds (*38*).
34. V. Y. Lee, R. Kato, M. Ichinohe, A. Sekiguchi, *J. Am. Chem. Soc.* **127**, 13142 (2005).
35. A. J. Ashe III, T. R. Diephouse, M. Y. El-Sheikh, *J. Am. Chem. Soc.* **104**, 5693 (1982).
36. M. J. Frisch *et al.*, Gaussian 03 revision D.02 (Gaussian, Wallingford, CT, 2004).
37. P. R. Schleyer, C. Maerker, A. Dransfeld, H. Jiao, N. J. R. E. Hommes, *J. Am. Chem. Soc.* **118**, 6317 (1996).
38. Z. Chen, C. S. Wannere, C. Corminboeuf, R. Puchta, P. v. R. Schleyer, *Chem. Rev.* **105**, 3842 (2005).

39. This work was partially supported by Grants-in-Aid for Scientific Research (no. 20038010 to M.S., no. 18066017 to S.N., and no. 19029037 to M.H.) in Priority Areas "Molecular Theory for Real Systems" and by the Nanotechnology Support Project from the Ministry of Education, Culture, Sports, Science, and Technology of Japan. M.S. acknowledges a research grant from Toray Science Foundation. Deposition nos. CCDC-750458 and 750459 contain the supplementary crystallographic data for compounds **1** and **4**, respectively. These data can be obtained free of charge at www.ccdc.cam.ac.uk/conts/retrieving.html (or from the Cambridge Crystallographic Data Centre, 12 Union Road, Cambridge CB2 1EZ, UK; fax, 44-1223-336-033; e-mail, deposit@ccdc.cam.ac.uk).

Supporting Online Material

www.sciencemag.org/cgi/content/full/328/5976/339/DC1
Methods
Reference

21 October 2009; accepted 11 December 2009
10.1126/science.1183648

A Fast Soluble Carbon-Free Molecular Water Oxidation Catalyst Based on Abundant Metals

Qiushi Yin,[1] Jeffrey Miles Tan,[1] Claire Besson,[1,2] Yurii V. Geletii,[1] Djamaladdin G. Musaev,[1] Aleksey E. Kuznetsov,[1] Zhen Luo,[1] Ken I. Hardcastle,[1] Craig L. Hill[1]*

Traditional homogeneous water oxidation catalysts are plagued by instability under the reaction conditions. We report that the complex $[Co_4(H_2O)_2(PW_9O_{34})_2]^{10-}$, comprising a Co_4O_4 core stabilized by oxidatively resistant polytungstate ligands, is a hydrolytically and oxidatively stable homogeneous water oxidation catalyst that self-assembles in water from salts of earth-abundant elements (Co, W, and P). With $[Ru(bpy)_3]^{3+}$ (bpy is 2,2′-bipyridine) as the oxidant, we observe catalytic turnover frequencies for O_2 production $\geq 5\ s^{-1}$ at pH = 8. The rate's pH sensitivity reflects the pH dependence of the four-electron O_2-H_2O couple. Extensive spectroscopic, electrochemical, and inhibition studies firmly indicate that $[Co_4(H_2O)_2(PW_9O_{34})_2]^{10-}$ is stable under catalytic turnover conditions: Neither hydrated cobalt ions nor cobalt hydroxide/oxide particles form in situ.

Producing renewable clean energy has become one of the most profound challenges of the 21st century (*1*). Most of the world's current energy supplies come from sunlight converted to chemical energy by plant photosynthesis. A central thrust of the current energy research focuses on artificial photosynthesis (*2*, *3*). Despite the intense global efforts to develop viable abiological water splitting systems, breakthroughs are needed in selectivity, speed, and stability of all three operational units: the sensitizer for light absorption and catalysts for water reduction and oxidation. Developing a viable water oxidation catalyst (WOC) has proven particularly challenging (*4*). An effective WOC must be fast; capable of water oxidation at a potential minimally above the thermodynamic value ($H_2O \rightarrow O_2 + 4H^+ + 4e^-$; $1.229 - 0.059 \times$ pH at 25°C); and, critically, stable to air, water, and heat (oxidative, hydrolytic, and thermal stability). There are many research groups working on heterogeneous and homogeneous WOCs. Heterogeneous WOCs generally have the advantages of low cost, ease of interface with electrode systems, and, critically, oxidative stability; but they are harder to study and thus optimize than homogeneous catalysts, and they tend to deactivate by surface poisoning or aggregation (*5*–*9*). Recently, Kanan and Nocera reported a robust heterogeneous WOC based on earth-abundant cobalt and phosphate (*8*), after earlier work by Creutz and Sutin (*10*), and demonstrated self-assembly under turnover conditions, a key to self-repair (*11*). More recently, the groups of Mallouk (*9*) and Frei (*12*) reported high catalytic water oxidation rates by using colloidal $IrO_2 \cdot nH_2O$ particles and Co_3O_4 (spinel) particles, respectively. In contrast, homogeneous WOCs are more amenable to spectroscopic, crystallographic, physicochemical, and computational investigation and thus more readily optimized. In addition, each individual molecule of a homogeneous catalyst is, in principle, capable of doing chemistry (a cost issue when precious metals such as Ru are involved). However, nearly all homogeneous catalysts contain organic ligands that are thermodynamically unstable with respect to oxidative degradation. As a result, all homogenous WOCs with organic ligands reported to date are oxidatively deactivated (*13*–*23*). A

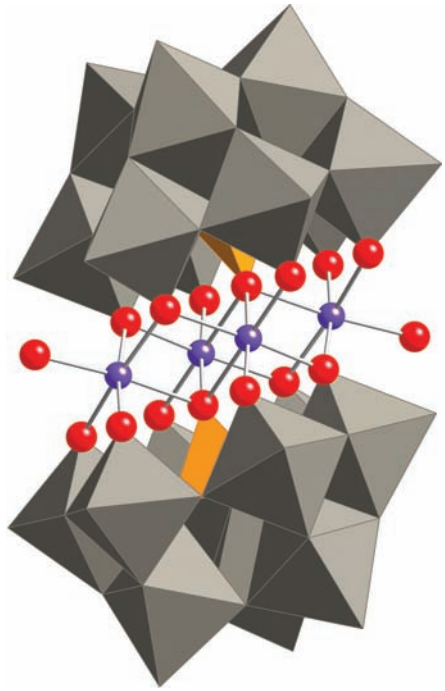

Fig. 1. X-ray structure of $\mathbf{Na_{10}}$-**1** in combined polyhedral ($[PW_9O_{34}]$ ligands) and ball-and-stick (Co_4O_{16} core) notation. Co atoms are purple; O/OH_2(terminal), red; PO_4, orange tetrahedra; and WO_6, gray octahedra. Hydrogen atoms, water molecules, and sodium cations are omitted for clarity.

[1]Department of Chemistry, Emory University, Atlanta, GA 30322, USA. [2]Institut Parisien de Chimie Moléculaire, UMR CNRS 7201, Université Pierre et Marie Curie Univ. Paris 06, Case 42, 4 place Jussieu, 75005 Paris, France.

*To whom correspondence should be addressed. E-mail: chill@emory.edu